Reproductive Sciences

Antenatal microbial colonization of mammalian gut

Journal:	*Reproductive Sciences*
Manuscript ID	RSCI-18-377.R2
Manuscript Type:	Original Manuscripts
Date Submitted by the Author:	14-Aug-2018
Complete List of Authors:	Borghi, Elisa; Università degli Studi di Milano, Dept. of Health Sciences Massa, Valentina; Università degli Studi di Milano, Dept. of Health Sciences Severgnini, Marco; Institute of Biomedical Technologies, National Research Council Fazio, Grazia; Centro Ricerca Tettamanti, Clinica Pediatrica, Dipartimento di Medicina e Chirurgia, Università degli Studi di Milano-Bicocca, Fondazione MBBM Avagliano, Laura; University of Milano, Obstetrics and Gynecology Menegola, Elena; Università degli Studi di Milano, Dipartimento di Scienze e Politiche Ambientali Bulfamante, Gaetano; Università degli Studi di Milano, Dept. of Health Sciences Morace, Giulia; Università degli Studi di Milano, Dept. of Health Sciences Borgo, Francesca; Università degli Studi di Milano, Dept. of Health Sciences
Keyword:	mammalian gut, embryonic development, microbiota, 16S rRNA gene sequencing
File Designation:	

Antenatal microbial colonization of mammalian gut

Elisa Borghi, PhD[1§], Valentina Massa, PhD[1§], Marco Severgnini, PhD[2], Grazia Fazio, PhD[3], Laura Avagliano, MD[1], Elena Menegola, PhD[4], Gaetano Bulfamante, MD[1], Giulia Morace, PhD[1], Francesca Borgo, PhD[1].

[§] These authors equally contributed to this work

[1] Dipartimento di Scienze della Salute, Università degli Studi di Milano, Milan, Italy; elisa.borghi@unimi.it, valentina.massa@unimi.it; laura.avagliano@unimi.it; gaetano.bulfamante@unimi.it; giulia.morace@unimi.it; francesca.borgo@unimi.it.

[2] Institute of Biomedical Technologies, National Research Council, Milan, Italy; marco.severgnini@itb.cnr.it

[3] Centro Ricerca Tettamanti, Clinica Pediatrica, Dipartimento di Medicina e Chirurgia, Università degli Studi di Milano-Bicocca, Fondazione MBBM, Monza, Italy; grazia.fazio@unimib.it

[4] Dipartimento di Scienze e Politiche Ambientali, Università degli Studi di Milano, Milan, Italy; elena.menegola@unimi.it

This work was done at the Università degli Studi di Milano, Milan, Italy

This study was funded by a Research Grant 2016 of the European Society of Clinical Microbiology and Infectious Diseases (ESCMID) and by Università degli Studi di Milano.

Corresponding author: Elisa Borghi, Dipartimento di Scienze della Salute, Università degli Studi di Milano, Milano, Italia.

Phone/Fax: +39 0250323287

Email: elisa.borghi@unimi.it

ABSTRACT

The widely accepted dogma of intrauterine sterility and initial colonization of the newborn during birth has been blurred by recent observations of microbial presence in meconium, placenta and amniotic fluid. Given the importance of a maternal-derived *in utero* infant seeding, it is crucial to exclude potential environmental or procedural contaminations, and to assess fetal colonization before parturition. To this end, we analyzed sterilely collected intestinal tissues, placenta and amniotic fluid from rodent fetuses, and tissues from autoptic human fetuses. Total bacterial DNA was extracted from collected samples and analyzed by Next Generation Sequencing techniques (NGS) using hyper-variable 16S rRNA regions (V3-V4). Colonizing microbes were visualized *in situ*, using labelled probes targeting 16S rDNA by fluorescent in situ hybridization (FISH).

NGS analysis showed the presence of pioneer microbes in both rat and human intestines, as well as in rodent placentas and amniotic fluids. Microbial communities showed fetus- and dam-dependent clustering, confirming the high inter-individual variability of commensal microbiota even in the antenatal period. Fluorescent *in situ* hybridization analysis confirmed the microbes' presence in the lumen of the developing gut. These findings suggest a possible antenatal colonization of the developing mammalian gut.

Keywords

mammalian gut, embryonic development, microbiota, 16S rRNA gene sequencing

Introduction

Fetus, amniotic fluid and chorioamnion tissue have long been considered sterile until birth or rupture of the amniotic sac. However, recent evidence shows that the intra-gestational sac environment harbors a diversity of microorganisms even in physiological pregnancies[1–3], contradicting the long-standing dogma of "womb sterility".[4] Indeed, the cultivable genera *Enterococcus, Streptococcus, Staphylococcus*, and *Propionibacterium* have been isolated from umbilical cord blood of healthy neonates born by caesarean section[5]. Within the abundant literature on human placenta microbiome composition[3,6,7], a recent study combining 16S ribosomal DNA-based and whole-genome shotgun metagenomic analyses, showed the presence of a unique placental microbiota, strongly resembling the maternal oral bacteria, with the dominance of *Firmicutes*, *Tenericutes, Proteobacteria, Bacteroidetes,* and *Fusobacteria* phyla[3]. In addition, amniotic fluid and placenta were found to have similar microbial communities, consistent across individuals[6]. Lactic acid bacteria and enteric bacteria have been reported in meconium collected after birth[8], and a certain degree of similarity has been demonstrated between meconium and amniotic fluid[6], probably related to liquid swallowing by the fetus during pregnancy.

All these data suggest that humans might come into contact with bacteria before birth, and, depending on the time of gestation and the type of bacteria that first seed the fetus, this antenatal colonization might have important physiological and clinical consequences. Indeed, microbes, either true pioneer or transient species, could expose the developing fetus to a diverse array of antigens[9] that educate the fetal immune system toward tolerance and participate in the full development of the gut-associated lymphoid tissue[10].

At the same time, toxins and viable microorganisms, through active and passive transport from maternal circulation to the placenta could gain direct entry into fetal circulation, eliciting infective and/or inflammatory processes[11].

Despite these recent advances in the field, a conclusive analysis of antenatal microbial colonization has not been reported[12], leaving a gap in the knowledge of this important developmental process. The present study is aimed at ascertaining antenatal microbial colonization of mammalian fetal intestinal tissues. To address this issue, a rodent animal model

was used to allow sterile experimental conditions. This was compared to human gut samples from fetal autopsies that were studied using a 16S rRNA amplicon-based NGS approach, validated by *in situ* detection.

Results

Microbial species are identifiable in rodent fetuses in utero

We collected, under sterile conditions, intestine, placenta and amniotic fluid from five rat fetuses: three fetuses (numbered 1-3) from one dam (dam A) and two (numbered 4-5) from the other (dam B). The tissues were analyzed by next generation sequencing.

An average of 259,465 reads were obtained per sample, giving a total of 4,670,364 reads overall. Paired-end reads generated from the original DNA fragments using Illumina MiSeq Next Generation Sequencing were merged and quality-filtered producing a total of 1,560,296 sequence tags from the gut samples, and 982,017 and 900,070 from placentas and amniotic fluids, respectively.

9 different bacterial phyla were identified in rat fetal samples following negative control subtraction. The most represented phyla (Fig. 1A), using a cut-off applied of a relative abundance greater than 1% in at least one experimental group, were *Firmicutes* (mean relative abundance ± SD, 57.0±8.6), *Bacteroidetes* (23.7±8.7), *Actinobacteria* (10.3±8.4), *Proteobacteria* (5.0±2.1), and *Verrucomicrobia* (2.8±1.9).

The most abundant families (Fig.1B) were: *Ruminococcaceae* (20.9±7.6), *Lachnospiraceae* (20.5±9.3), *Bacteroidaceae* (11.4±4.4), *Veillonellaceae* (5.9±3), *Rikenellaceae* (4.2±2.3), and *Propionibacteriaceae* (3.5±6.3).

Microbial community is characteristic of fetuses and dams

In order to understand the main determinants constituting the microbial diversity, we evaluated the differences amongst the samples on both richness and composition. Tissues (i.e. intestine, placenta, and amniotic fluid), dams (i.e.: A and B) and fetuses were considered for microbiota profiling. The analysis of samples biodiversity (α-diversity) showed clustering according to dam and

fetus rather than analyzed tissue. Faith's phylogenetic diversity (Fig. 2), measured based on distances, and observed species metrics showed a significant separation dependent on fetus (Mann-Whitney test: p=0.016 and 0.019, respectively). Both the metrics showed a separation dependent also on dam (permutation-based test: p=0.004 and 0.036, respectively). Interestingly, no significant separation was observed based on tissue type (p>0.05), independently from the metric used to compare distributions.

To evaluate whether different samples were characterized by distinct microbiota composition profiles (β-diversity, Fig. 3A), the distribution of Unifrac distances was assessed. Both unweighted, which gives equal importance to rare and common taxa, and weighted Unifrac distances, which gives a higher importance to the most abundant bacteria, were used.

As with the α-diversity, the β-diversity analyses clustered according to fetus (adonis test p=0.009 and 0.006 on unweighted and weighted Unifrac distances, respectively) and to dam (adonis test p=0.015 on weighted Unifrac distances).

Distributions of unweighted Unifrac distances (Fig. 3B) on fetus were statistically different (p=0.01), whereas weighted Unifrac distances were not (p=0.09), indicating that significant differences are present in sub-dominant components of the microbiota. In detail, fetus 1 was characterized by a high relative abundance of *Propionibacteriaceae* (14.3% compared to an average of 1.1% in other fetuses) and *Corynebacteriaceae* (4.1% compared to an average of 0.4% in other fetuses). fetus 3 showed an increased abundance of *Erysipelotrichaceae* (1.7% compared to an average of 0.9% in other fetuses), and fetus 5 was enriched in *Porphyromonadaceae* (average relative abundance 2.4% compared to 1.0% in other fetuses) (Suppl. Fig. 1 and Suppl. Fig. 2A).

Analysis of observed species metric (p=0.036) and Faith's phylogenetic distances (p=0.004) allowed for a significant separation among dams, with dam B presenting with a lower biodiversity (Suppl. Fig 3).

Analysis of distances based on sample origin (i.e. fetus, tissue and dam) showed a trend indicating similarity in microbial profiles among fetuses (Fig. 3C).

The microbiota signature for each tissue appeared less distinct, with only some hints of a lower presence of *Verrucomicrobiaceae* in placenta tissue (relative abundance: 1.1% compared to 2.7%

and 3.7% in amniotic fluid and intestine, respectively) and a trend of higher relative abundance of *Barnesiellaceae* in the intestine (4.0% compared to 1.4% and 1.5% in placenta and amniotic liquid, respectively) (Suppl. Fig. 2C and Suppl. Fig. 4). Few differences emerged in the comparison between dam A and B (Suppl. Fig. 2B and Suppl Fig. 5).

Bacteria are visualised in the gut during rodent fetal development

To assess bacteria distribution, *in situ* analysis was performed on whole sectioned fetuses. Fluorescent detection revealed the presence of bacteria in the gut lumen of developing rat fetuses (Fig. 4A and 4B). In particular, eubacteria (green fluorescence) could be visualized on the different analyzed sections, confirming that bacteria colonize the rodent intestine before birth. Probe for *Staphyloccaceae* did not give positive fluorescent signal in any of the tissue sections analyzed.

Bacteria are present in the gut during human fetal development

Paraffin-embedded intestinal tissues from three third trimester (gestational age 29, 31 and 33 weeks) human fetuses were screened for the presence of fetal microbiota.

In all analyzed samples, bacteria were observed. The most represented phyla (Fig. 5A) were *Firmicutes* (57.3±4.5), *Bacteroidetes* (17.4±1.2), *Actinobacteria* (16.8±5.4), *Proteobacteria* (4.9±2.2), and *Verrucomicrobia* (2.7±1.7). At family level, the most abundant taxa were: *Lachnospiraceae* (19.0±8.6), *Ruminococcaceae* (18.2±2.4), *Propionibacteriaceae* (9.1±4.1), *Bacteroidaceae* (8.9±2.2), *Streptococcaceae* (4.7±1.7), and *Veillonellaceae* (4.7±0.6).

The presence of bacteria indicated by the data obtained by NGS analysis was further validated by visualizing eubacteria in the lumen of the developing gut by fluorescent *in situ* hybridization (Fig. 5B).

DISCUSSION

The presence of a meconium microbiota supports the existence of maternal microbial transmission *in utero*[8]. In this study, we show that bacteria are present in anatomical fetal mammalian gut

sections. Reported relative abundance in meconium[6,8,13] indicate a consistent presence of *Proteobacteria*, whereas in this study, both in human and rat developing gut, *Firmicutes* were found to be more represented. These changes in microbiota may be a consequence of physiological changes that occur during birth. The present study does not suffer for the rodent (not the human) sampling of the known different oxygen levels given the immediate freezing of dissected tissues.

Supporting the important role of the microbiota community in the developing mammalian gut, the phyla composition found in analyzed samples (*Firmicutes, Bacteroidetes, Actinobacteria, Proteobacteria* and *Verrucomicrobia*) closely resembles those reported in healthy adult human gut[14,15]. It is important to note that, compared to adult and childhood tissues[16,17], the developing gut is enriched in *Actinobacteria*, and depleted in *Bacteroidetes*. *Actinobacteria* abundance has been shown to progressively increase in infant feces during lactation and to then decrease when solid food is introduced in the diet. The opposite has been reported for *Bacteoidetes*[18–20]. Hence, the difference between fetal and adult gut composition is in line with infant fecal microbiota, suggesting that solid food might be responsible for the switch. It could also suggest that the presence of a maternally provided reservoir of bifidobacteria, that with human milk oligosaccharides are known to be fundamental for the development of a balanced infant microbiota and a fully functional gastrointestinal tract [18,21–23].

Another difference found in our study compared to bacteria composition reported in meconium collected after birth[6,8], is that *Staphylococcaceae* and *Streptococcaceae* appear to be less abundant during uterine life. It is known that staphylococci are characteristic of higher respiratory tract and skin microbiota, hence it is conceivable that colonization occurs during birth or from the first days of life through contact with maternal tissues. It has also recently been shown that both genera are abundant in colostrum and maternal milk[24], indicating a possible dual colonizing path. Analysis of 16S rRNA amplicon data showed that microbiota composition is fetus- and dam-specific rather than tissue specific. Indeed, bacterial families found in amniotic fluid and placenta overlap with those found in the corresponding fetus. Importantly, the specificity seems to be independent of growing environment (i.e., uterine tissues etc.) but it seems to relate to micro

niches (i.e. embryonic implant). This is true not only for the microbial community, but also for other developmental determinants, such as genetic, metabolic, biochemical or epigenetic components known to be specific to the single developing organism and not always shared among all siblings. This is in addition to the possible confounding factors of gender, time and site of implantation etc. Given that bacteria colonize mammalian gut during intrauterine life, the fundamental question remains as to the source and the path of this *in utero* seeding or exposure. Recent findings[3] have described how, analyzing a significant number of placentas collected after birth, the placental microbiota shares more similarities with that of the oral composition compared to vaginal, skin and/or gut communities. Rather than identifying the origin of placental microbiota, these data support the exclusion of a passive dispersion through excreting organs. In the literature, a possible microbiota colonization *in utero* has been often hypothesized as a consequence of pathogens known to be able to reach the developing fetus. Our data suggest an alternative mechanism, where pathogens may pass the maternal barrier as a consequence of the necessary permissiveness to commensal bacteria[4], instead of resulting from infectious events (reviewed in Doran *et al.*[25]).

Clearly, considering the accumulating evidence for a strict relationship between microbiome and health status, in all studied settings (age, gender, ethnicity, mtDNA SNP, haplogroup, etc.)[26–31] and the importance of maintaining or replenishing the microbial community in pathological conditions[29,32,33], the present paper reports data contributing to the open field of investigation relating to the management of healthy pregnancies[34]. Future studies will be devoted to overcome the limitations of the present research, i.e. prospective collection of fetal human samples, increase number of rodent fetuses, and implementing culture techniques for growing commensal microorganisms.

MATERIALS AND METHODS

Animals and housing

CD albino rats (Sprague-Dawley) were maintained in standard conditions (light 6am-6pm, T=22+/-2°C, humidity = 55+/-5%) with tap water and food (Mucedola standard diet) *ad libitum*. Virgin

females were caged overnight with males of proven fertility. The day of positive vaginal smear was considered as day 0. The pregnant rats were housed individually. Animals were euthanized by carbon dioxide inhalation and bilaterally pregnant uterine samples were collected in the morning of gestational day 16. Amniotic fluid, placenta and fetal intestines were dissected, collected in sterile conditions, and stored at -80°C until use. For dissection, uteruses were placed in sterile saline solution under laminar flow cabinet, and all procedures were conducted in the hood using UV sterilized equipment within a sterile field created by a Bunsen burner, until samples were placed in sterile tubes. For *in situ* hybridization, whole fetuses were collected in paraformaldehyde 4% (v/v), and kept at 4°C in rotation for 4 days. Samples were then washed twice in phosphate saline solution (PBS), rehydrated through a graded series of alcohols, and paraffin-embedded.

All animal procedures were conducted in accordance with the ethical guidelines approved by the University of Milan in compliance with national (Dlgs 26/2014) and international laws and policies (EEC Council Directive 86/609).

Human samples

Human samples were included based on stillborn non-macerated fetuses and of gut tissue availability. The three fetuses were not malformed and with normal karyotype. Pregnancies were reported as uneventful, including infection and inflammation disease or premature rupture of the membranes, until intrauterine fetal death. Autopsy was performed following international protocols[35].

4 µm thick tissue sections from formalin-fixed, paraffin-embedded tissue samples were cut and processed for *in situ* hybridization by deparaffinization in xylene and rehydration through a graded series of alcohols. For NGS analysis, tissue sections, cut under laminar flow cabinet using sterile blades and placed in sterile tubes, were washed twice with 1 mL of Histo-Clear (Sigma Aldrich, Milan, Italy) for 15 minutes with rotation at 56°C or until diaphanization. Tissue was recovered by centrifugation, washed in ethanol and dried for DNA extraction.

The study was exempt from Institutional Review Board approval because, following Italian Data Protection Act 9/2013, autopsy material sampled for diagnostic purposes can be used for research

as long as patient privacy is ensured. This law is in line with European Commission recommendation n. Rec(2006)4.

Next Generation Sequencing analysis

Total bacterial DNA extraction was performed using the QIAamp DNA Microbiome Kit (QIAGEN, Hilden, Germany), following manufacturer's instructions. Particular attention was paid to avoid environmental contamination of collected samples, and cross-contamination between samples. Samples were individually processed for DNA extraction under laminar flow cabinet, following UV sterilization. Empty tubes, processed in parallel during tissue recovery and DNA extraction, were used as negative controls. A number of corrective measures have been applied. In particular, UV radiation of surfaces and instruments, use of disposable equipment or autoclave-based sterilization. Negative controls were run in parallel and processed for detecting possible contaminating microorganisms. 16s rRNA sequencing results did not show commonly reported environmental and reagent contaminants[36].

16S rRNA gene amplicon libraries were performed with a two-step barcoding approach according to Illumina 16S Metagenomic Sequencing Library Preparation (Illumina, San Diego, CA, USA), which amplifies two hypervariable regions (i.e.: V3, V4) of the 16S rRNA bacterial gene. Library concentration and exact product size were measured using a KAPA Library Quantification Kit (Kapa Biosystems, Woburn, MA, USA) and Agilent 2100 Bioanalyzer System (Agilent, Santa Clara, CA, USA), respectively. Agilent analysis for evaluating the correct predicted size of amplicons showed no bands in negative controls, extracted and processed in parallel with samples (Suppl Fig 6). Prior to sequence, libraries were pooled using Amicon Ultra 0.5ml Centrifugal Filters (Merck Millipore Ltd, Tullagreen, Carrigtwohill Co, Cork, Ireland).

The resulting library was loaded on a MiSeq® 500 cycle-v2 cartridge to obtain a paired-end 2×250 bp sequencing. Demultiplexed FASTQ files were generated by Illumina MiSeq Reporter and 2.5 Gbases were obtained.

Raw sequence data determined in this study are available at NCBI Short Read Archive (SRA, https://www.ncbi.nlm.nih.gov/sra/) under Accession numbers PRJNA379373 and PRJNA379370.

Fluorescence** in situ **hybridization (FISH) analysis

Paraffin-embedded tissue specimens (4 μm thick) were deparaffinized by sequential steps in xylene. Then samples were re-hydrated in 95% ethanol, 90% ethanol, and finally deionized water. The slides were air-dried prior to hybridization.

FISH probe sequences for Eubacteria (EUB 338-I, 5'-GCTGCCTCCCGTAGGAGT-3'; EUB 338-III, 5'-GCTGCCACCCGTAGGTGT-3'), encompassing all bacterial species in Bacteria domain (labelled with FITC), *Bacteroides* (BAC303, 5'-TCCTCCATATCTCTGCGC-3', Cy3), and *Lachnospiraceae* (LACHNO, 5'-TTCCCATCTTTCTTGCTGGC-3', Cy5) were obtained from probeBase website[37]. Negative control probe (complementary to EUB 338-I probe, NON-EUB, 5'-ACTCCTACGGGAGGCAGC-3') was also hybridized to evaluate non-specific binding. *Staphylococcaceae* probe (STAPHY, 5'-TCCTCCATATCTCTGCGC-3', Cy3) sequence was designed as described by Gey et al.[38], and used to assess possible environmental contaminants in sampling. Probes were purchased from Integrated DNA Technologies (IDT, San Jose, CA, USA). Hybridization was carried out using standard methods[38,39]. Briefly, sections were deparaffinized and rehydrated in serial solutions. Following section air-drying, specific oligonucleotide probes were hybridized using conditions optimized for each probe for stringent hybridizations: BAC303 at 48°C and 10% formamide; STAPHY, and LACHNO at 48°C and 30% formamide; EUB 338-I, and EUB 338-III, at 48°C and 10% or 30% formamide according to the paired probes.

DAPI (4',6-diamidino-2-phenylindole) counterstaining was applied to assess prokaryotic and eukaryotic nuclear morphology.

In this set of experiments, a number of controls were used: sections hybridized with STAPHY probe, that resulted negative, to exclude common contaminants; sections hybridized with NON-EUB probe, as negative control; artificially contaminated sections hybridized with STAPHY probe, that resulted positive, as technical control.

Images of probe-labelled sections were acquired using a confocal laser scanning microscope (CLSM, TCS SP2, Leica, Wetzlar, Germany). Microorganisms were checked for position, size and morphology. Confocal images were acquired by series and sequential scan mode. Photomultiplier

tube detectors were adjusted to minimize the bleed-through of fluorescent emissions and to optimize signal/noise ratio, in particular versus tissue autofluorescence.

Data analysis

Sequencing reads were processed, filtered and analyzed following similar procedures described in Borghi et al.[40]. Briefly, read pairs were merged together by PandaSeq software[41] discarding fragments of length <300 bases or >900 bases, as well as non-overlapping sequences. Then, fragments were quality-filtered, clustered into OTUs (Operational Taxonomic Units) and taxonomically classified against the 13.8 release of the Greengenes bacterial 16S rRNA database (http://greengenes.lbl.gov) using the QIIME suite (v. 1.8.0[42]).

Biodiversity (α-diversity) was evaluated by permutation-based t-tests, whereas "adonis" of the R package "vegan" was used for bacterial composition (β-diversity). In addition, due to the reduced number of samples per category, we devised an alternative strategy for comparing the distributions of distances within and between each experimental group for both α-diversity and β-diversity evaluations. Each sample was assigned to an experimental group according to one of the associated labels (i.e.: tissue type, dam or fetus number); then, a distance between each sample and all the others was calculated. This allowed distinguishing distances between samples belonging to the same ("intra-category" distance) or to a different ("inter-category" distance) experimental group. This strategy was applied for evaluating the absolute difference for α-diversity indexes (i.e.: chao1, Shannon index, observed species and Faith's phylogenetic distance) and the weighted or unweighted Unifrac distances[43] (β-diversity). A Mann-Whitney U-test was applied for comparing the distributions of "intra-" and "inter-category" distances.

Details of statistical methods are provided as Supplementary information.

ACKNOWLEDGMENTS: This study was funded by a Research Grant 2016 of the European Society of Clinical Microbiology and Infectious Diseases (ESCMID) to F.B, and by Università degli Studi di Milano. We thank Raffaella Adami for her assistance in confocal laser microscopy

techniques, Francesca Di Renzo and Silvia Rigamonti for technical assistance. We are grateful to Ms Dawn Savery and Dr Jon Wilson for commenting on the manuscript.

AUTHOR CONTRIBUTIONS: E.B., V.M. and F.B. conceived and designed the study; E.M and V.M. performed rodent housing and sampling; L.A. and G.B. performed human tissue sampling; E.B. F.B. and G.F. performed experiments**;** M.S. performed bioinformatics analysis; M.S., E.B. and F.B. analysed the data; V.M. and E.B. wrote the paper. All authors made comments on the manuscript; G.M. supervised the project.

COMPETING FINANCIAL INTERESTS: The authors declare no conflict of interest.

REFERENCES

1. Brugman S, Perdijk O, van Neerven RJJ, Savelkoul HFJ. Mucosal Immune Development in Early Life: Setting the Stage. *Arch Immunol Ther Ex*. 2015; 63: 251–268.
2. Ardissone AN, de la Cruz DM, Davis-Richardson AG, et al. Meconium microbiome analysis identifies bacteria correlated with premature birth. *PLoS One*. 2014; 9: e90784.
3. Aagaard K, Ma J, Antony KM, Ganu R, Petrosino J, Versalovic J. The placenta harbors a unique microbiome. *Sci Transl Med.* 2014; 6: 237ra65.
4. Funkhouser LJ, Bordenstein SR. Mom Knows Best: The Universality of Maternal Microbial Transmission. *PLoS Biol.* 2013; 11: 1–9.
5. Jiménez E, Fernández L; Marín ML*,* et al*.* Isolation of commensal bacteria from umbilical cord blood of healthy neonates born by cesarean section. *Curr Microbiol.* 2005; 51: 270–274.

6. Collado MC, Rautava S, Aakko J, Isolauri E, Salminen S. Human gut colonisation may be initiated in utero by distinct microbial communities in the placenta and amniotic fluid. *Sci Rep.* 2016; 6: 23129.

7. Prince AL, Ma J, Kannan PS, et al. The placental membrane microbiome is altered among subjects with spontaneous preterm birth with and without chorioamnionitis. *Am J Obstet Gynecol.* 2016; 214**:** 627e1-627e16.

8. Jiménez E, Marín ML, Martín R, et al. Is meconium from healthy newborns actually sterile? *Res Microbiol.* 2008; **159:** 187–193.

9. Avagliano L, Marconi AM, Candiani M, Barbera A, Bulfamante G. Thrombosis of the umbilical vessels revisited. An observational study of 317 consecutive autopsies at a single institution. *Hum Pathol.* 2010; 41: 971–979.

10. Belkaid Y, Hand TW. Role of the microbiota in immunity and inflammation. *Cell*. 2014; 157: 121–141.

11. Fardini Y, Chung P, Dumm R, Joshi N, Han YW. Transmission of diverse oral bacteria to murine placenta: Evidence for the oral microbiome as a potential source of intrauterine infection. *Infect Immun.* 2010; 78: 1789–1796.

12. Perez-Muñoz ME, Arrieta MC, Ramer-Tait AE, Walter J. A critical assessment of the 'sterile womb' and 'in utero colonization' hypotheses: implications for research on the pioneer infant microbiome. *Microbiome*. 2017; 5: 48.

13. Chu DM, Ma J, Prince AL, Antony KM, Seferovic MD, Aagaard KM. Maturation of the infant microbiome community structure and function across multiple body sites and in relation to mode of delivery. *Nat Med.* 2017; 23: 314-326.

14. Huttenhower C, Human Microbiome Project Consortium. Structure, function and diversity of the healthy human microbiome. *Nature*. 2012; 486: 207–14.

15. Qin J, Li R, Raes J, et al. A human gut microbial gene catalogue established by metagenomic sequencing: Commentary. *Nature*. 2010; 11: 28.

16. Greenhalgh K, Meyer KM, Aagaard KM, Wilmes P. The human gut microbiome in health: establishment and resilience of microbiota over a lifetime. *Env Microbiol.* 2016; 18: 2103–

2116.

17. Riva A, Borgo F, Lassandro C, et al. Pediatric obesity is associated with an altered gut microbiota and discordant shifts in *Firmicutes* populations. *Env Microbiol.* 2016; 19: 1–29.

18. Turroni F, Ribbera A, Foroni E, van Sinderen D, Ventura M. Human gut microbiota and bifidobacteria: From composition to functionality. *Antonie van Leeuwenhoek,* 2008; 94: 35–50.

19. Scott KP, Gratz SW, Sheridan PO, Flint HJ, Duncan SH. The influence of diet on the gut microbiota. *Pharmacol Res.* 2012; 69: 52-60.

20. Koenig JE, Spor A, Scalfone N, et al. Succession of microbial consortia in the developing infant gut microbiome. *Proc Natl Acad Sci USA.* 2011; Suppl 1:4578-85.

21. Asakuma S, Hatakeyama E, Urashima T, et al. Physiology of consumption of human milk oligosaccharides by infant gut-associated bifidobacteria. *J Biol Chem.* 2011; 286: 34583–34592.

22. Wang M, Li M, Wu S, et al. Fecal microbiota composition of breast-fed infants is correlated with human milk oligosaccharides consumed. *J Pediatr Gastroenterol Nutr.* 2015; 60: 825–833.

23. Rasmussen SO, Martin L, Østergaard MV, et al. Human milk oligosaccharide effects on intestinal function and inflammation after preterm birth in pigs. *J Nutr Biochem.* 2017; 40: 141–154.

24. Drago L, Toscano M, De Grandi R, Grossi E, Padovani EM, Peroni DG. Microbiota network and mathematic microbe mutualism in colostrum and mature milk collected in two different geographic areas: Italy versus Burundi. *ISME J.* 2016; 11: 1–10.

25. Doran KS, Banerjee A, Disson O, Lecuit M. Concepts and mechanisms: Crossing host barriers. *Cold Spring Harb Perspect Med.* 2013; **3:** 1–20.

26. Hullar MAJ, Fu BC. Diet, the gut microbiome, and epigenetics. *Cancer J.* 2014; 20: 170–5.

27. De Filippo C, Cavalieri D, Di Paola M, et al. Impact of diet in shaping gut microbiota revealed by a comparative study in children from Europe and rural Africa. *Proc Natl Acad Sci USA.* 2010; 107: 14691–6.

28. Strati F, Di Paola M, Stefanini I, et al. Age and gender affect the composition of fungal population of the human gastrointestinal tract. *Front Microbiol.* 2016; 7: 1–16.

29. Lozupone CA, Stombaugh JI, Gordon JI, Jansson JK, Knight R. Diversity, stability and resilience of the human gut microbiota. *Nature*. 2012; 489: 220–230.

30. Aagaard K, J Petrosino J, Keitel W, et al. The Human Microbiome Project strategy for comprehensive sampling of the human microbiome and why it matters. *FASEB J.* 2013; 27: 1012–1022.

31. Ma J, Coarfa C, Qin X, et al. mtDNA haplogroup and single nucleotide polymorphisms structure human microbiome communities. *BMC Genomics*. 2014; 15: 257.

32. Clemente J C, Ursell LK, Parfrey LW, Knight R. The impact of the gut microbiota on human health: An integrative view. *Cell*. 2012; 148: 1258–1270.

33. Peterson CT, Sharma V, Elmén L, Peterson SN. Immune homeostasis, dysbiosis and therapeutic modulation of the gut microbiota. *Clinical Exp Immunol.* 2015; 179: 363–377.

34. Mueller NT, Bakacs E, Combellick J, Grigoryan Z, Dominguez-Bello MG. The infant microbiome development: mom matters.Trends Mol Med. 2015; 21: 109–117.

35. Mecacci F, Serena C, Avagliano L et al. Stillbirths at Term: Case Control Study of Risk Factors, Growth Status andPlacental Histology. *PLoS One*. 2016;11(12):e0166514.

36. Salter SJ, Cox MJ, Turek EM et al. Reagent and laboratory contamination can critically impact sequence-based microbiome analyses. *BMC Biol*. 2014;12:87.

37. Greuter D, Loy A, Horn M, Rattei T. ProbeBase-an online resource for rRNA-targeted oligonucleotide probes and primers: New features 2016. *Nucleic Acids Res.* 2016; 44: D586–D589.

38. Gey A, Werckenthin C, Poppert S, Straubinger RK. Identification of pathogens in mastitis milk samples with fluorescent in situ hybridization. *J Vet Diagn Invest.* 2013; 25: 386–394.

39. Berry D, Schwab C, Milinovich G,et al. Phylotype-level 16S rRNA analysis reveals new bacterial indicators of health state in acute murine colitis. *ISME J.* 2012; 6: 2091–106.

40. Borghi E, Borgo F, Severgnini M, Savini MN, Casiraghi MC, Vignoli A. Rett Syndrome: A Focus on Gut Microbiota. *Int J Mol Sci.* 2017; 18: 344.

41. Masella AP, Bartram AK, Truszkowski JM, Brown DG, Neufeld JD. PANDAseq: paired-end assembler for Illumina sequences. *BMC Bioinformatics*. 2012; 13: 31.

42. Caporaso JG, Kuczynski J, Stombaugh J, et al. QIIME allows analysis of high-throughput community sequencing data. *Nat Methods*. 2010; 7: 335–6.

43. Lozupone C, Knight R. UniFrac: A new phylogenetic method for comparing microbial communities. *Appl Environ Microbiol.* 2005; 71: 8228–8235.

FIGURE LEGENDS

Figure 1- *Pioneer microbiota in the developing rodent gut*

Bar charts representing the relative abundance of 5 fetal intestines (I1-I5), amniotic fluids (A1-A5) and placentas (P1-P5). The figure shows relative abundance of bacterial **(A)** phyla and **(B)** families.

Figure 2- *Microbial biodiversity (α-diversity) is fetus-specific*

(A) α-diversity rarefaction curves according to Faith's phylogenetic distance ("PD whole tree"). X-axis reports the number of sequences per sample, whereas Y-axis shows the value of the metric. Samples are grouped based on fetus number. **(B)** Distribution of distances between **α**-diversity PD whole tree values; distances are labelled as "intra-" or "inter-category" according to fetus number. Dashed black line represents the mean of the distances, whereas the solid black line represents the median.

Figure 3- *Microbiota composition (β-diversity) is fetus-specific*

(A) Principal coordinates analysis (PCoA) of the unweighted Unifrac distances; PCoA components 1 and 3 are reported. Samples are connected together on the basis of fetus number. **(B)** Boxplots of intra- and inter-category unweighted Unifrac distances among samples; categories

are based on the fetus number. **(C)** Boxplots of intra-category weighted Unifrac distances among samples; samples are grouped according to fetus, tissue or dam.

Figure 4- *Eubacteria in the developing rodent gut lumen*

Confocal microscopy images showing **(A)** eubacteria (in green) in the lumen of a 16 days post coitum rat fetus; **(B)** at a higher magnification (inset is represented as a white box in A) note the typical bacterial morphology and it is possible to identify few *Bacteroides* spp. (yellow). In blue is DAPI (nuclei) and 50 μm scale bar is reported in B. Asterisks indicate bacterial cells.

Figure 5- *Eubacteria in the developing human gut*

(A) Bar charts representing the family relative abundance at family level of three fetal human intestines (29, 31, and 33 weeks of gestation, respectively). **(B)** Representative confocal microscopy images of *in situ* hybridization showing the presence of eubacteria (in green-, inset showing higher magnification) in the lumen human fetuses. In blue is DAPI (nuclei) and 100 μm and 50 μm (inset) scale bars are reported. Asterisks indicate bacterial cells.

Supplementary figure 1- Relative abundance of most represented bacterial families (per fetus)

Plots show relative abundances of the main 20 bacterial families separated by fetus number. Values corresponding to the same tissue (i.e. intestine, amniotic fluid, and placenta) are represented by the same color (red, green and blue, respectively). The solid black line represents the median of the values per each fetus, whereas the dashed black line shows the average.

Supplementary figure 2 – Average relative abundance of tissue, dam and fetus microbiota

Average relative abundance of the main microbial families in (A) fetuses, (B) dams and (C) tissues. Samples considered for the analysis were 3 for each fetus, 9 for dam A, 6 for dam B and 5 for each tissue.

Supplementary figure 3- Dam-effect on microbiota

(A) Principal coordinates analysis (PCoA) of the weighted Unifrac distances; PCoA components 1 and 3 are reported. Samples are grouped based on dam. (B) Y-axis depicts α-diversity rarefaction curves according to Faith's phylogenetic distance (PD whole tree); numbers of sequences per sample are reported on X-axis. (C) Boxplots of intra- and inter-category unweighted Unifrac distances among samples; categories are based on dam.

Supplementary figure 4- Relative abundance of most represented bacterial families (per tissue)

Plots show relative abundances of the main 20 bacterial families separated by tissue type. Values corresponding to the same fetus are represented by the same color. The solid black line represents the median of the values per each tissue, whereas the dashed black line shows the average.

Supplementary figure 5- Relative abundance of most represented bacterial families (per dam)

Plots of relative abundances of the main 20 families of the microbiota separated on dam. Relative abundance corresponding to intestine, amniotic fluid and placenta are represented in red, green and blue, respectively. The solid black line represents the median of the values per each dam, whereas the dashed black line shows the average.

Supplementary figure 6- Representative electrophoresis of 16S amplicons during library check

Agilent 2100 Bioanalyzer system was used to assess exact product size and quantity of amplicons after 16S rRNA gene library preparation, using Agilent DNA 1000 Kit, for the separation, sizing and quantification of dsDNA fragments from 25 to 1000 bp (Agilent Technologies, Santa Clara, CA, USA). First lane (L), molecular weight ladder; lines 1 and 2, negative controls (empty tubes that

have been processed in parallel during tissue recovery and DNA extraction); lines 3 to 12, human and rat samples. Upon sequencing, a number of reads to the limit of detection, despite the technical concentration step, has been obtained for negative controls. Known environmental contaminants were never observed.

Figure 1- Pioneer microbiota in the developing rodent gut
Bar charts representing the relative abundance of 5 fetal intestines (I1-I5), amniotic fluids (A1-A5) and placentas (P1-P5). The figure shows relative abundance of bacterial (A) phyla and (B) families.

220x200mm (300 x 300 DPI)

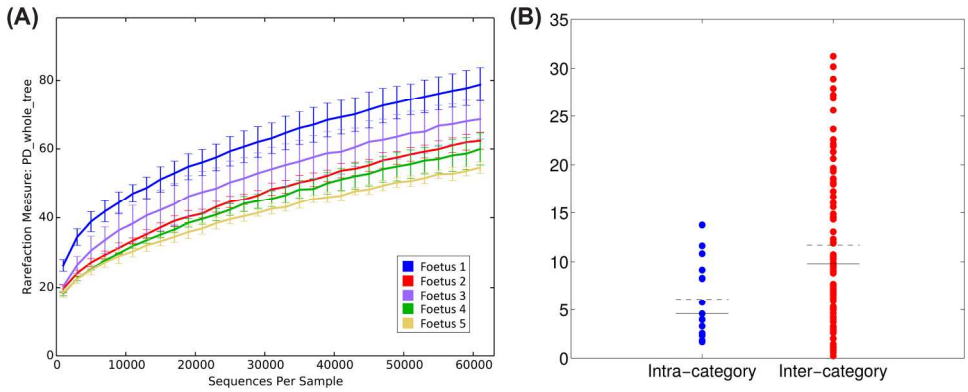

Figure 2- Microbial biodiversity (α-diversity) is fetus-specific
(A) α-diversity rarefaction curves according to Faith's phylogenetic distance ("PD whole tree"). X-axis reports the number of sequences per sample, whereas Y-axis shows the value of the metric. Samples are grouped based on fetus number. (B) Distribution of distances between α-diversity PD whole tree values; distances are labelled as "intra-" or "inter-category" according to fetus number. Dashed black line represents the mean of the distances, whereas the solid black line represents the median.

209x84mm (300 x 300 DPI)

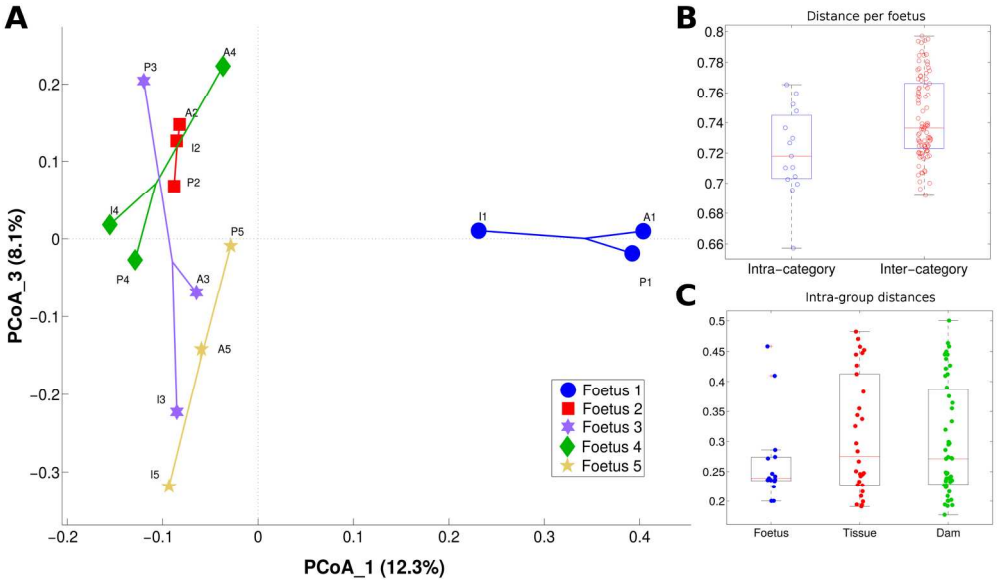

Figure 3- Microbiota composition (β-diversity) is fetus-specific
(A) Principal coordinates analysis (PCoA) of the unweighted Unifrac distances; PCoA components 1 and 3 are reported. Samples are connected together on the basis of fetus number. (B) Boxplots of intra- and inter-category unweighted Unifrac distances among samples; categories are based on the fetus number. (C) Boxplots of intra-category weighted Unifrac distances among samples; samples are grouped according to fetus, tissue or dam.

209x122mm (300 x 300 DPI)

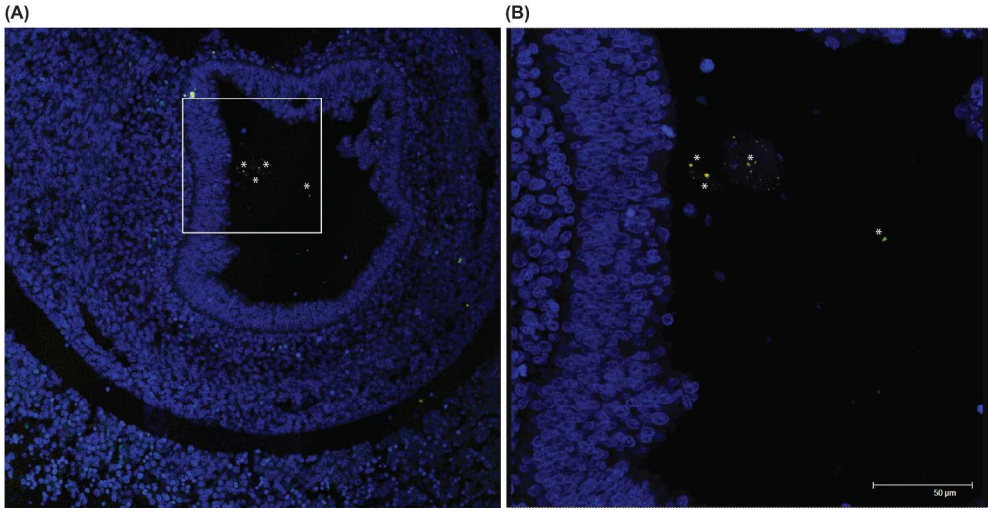

Figure 4- Eubacteria in the developing rodent gut lumen
Confocal microscopy images showing (A) eubacteria (in green) in the lumen of a 16 days post coitum rat fetus; (B) at a higher magnification (inset is represented as a white box in A) note the typical bacterial morphology and it is possible to identify few Bacteroides spp. (yellow). In blue is DAPI (nuclei) and 50 µm scale bar is reported in B. Asterisks indicate bacterial cells.

273x139mm (300 x 300 DPI)

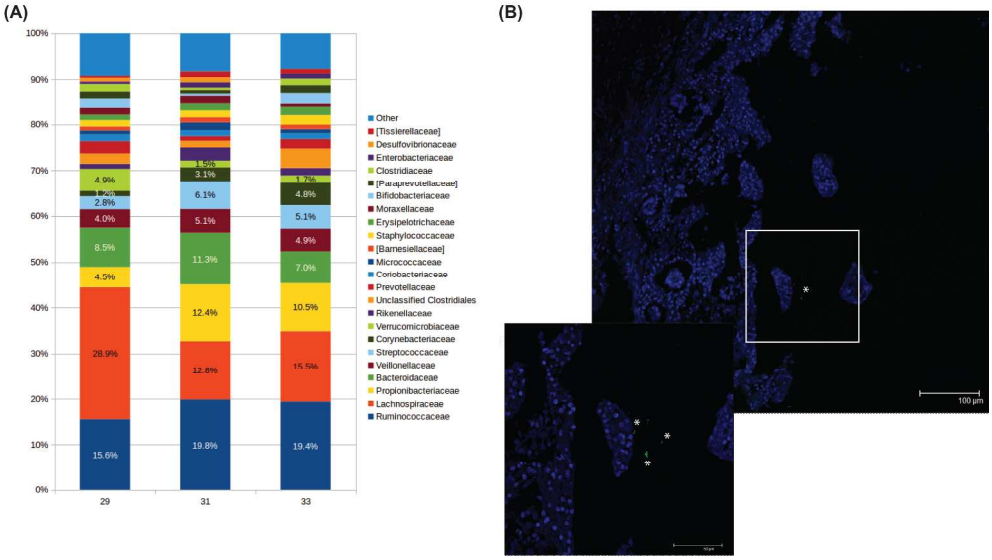

Figure 5- Eubacteria in the developing human gut
(A) Bar charts representing the family relative abundance at family level of three fetal human intestines (29, 31, and 33 weeks of gestation, respectively). (B) Representative confocal microscopy images of in situ hybridization showing the presence of eubacteria (in green-, inset showing higher magnification) in the lumen human fetuses. In blue is DAPI (nuclei) and 100 µm and 50 µm (inset) scale bars are reported. Asterisks indicate bacterial cells.

280x156mm (300 x 300 DPI)

SUPPORTING INFORMATION

ANTENATAL MICROBIAL COLONISATION OF MAMMALIAN GUT

Elisa Borghi[1§*], Valentina Massa[1§], Marco Severgnini[2], Grazia Fazio[3], Laura Avagliano[1], Elena Menegola[4], Gaetano Bulfamante[1], Giulia Morace[1], Francesca Borgo[1]

[1] *Dipartimento di Scienze della Salute, Università degli Studi di Milano, 20142 Milan, Italy;*
[2] *Institute of Biomedical Technologies, National Research Council, 20090 Segrate, Italy;*
[3] *Centro Ricerca Tettamanti, Clinica Pediatrica, Dipartimento di Medicina e Chirurgia, Università degli Studi di Milano-Bicocca, Fondazione MBBM, Monza, Italy*
[4] *Dipartimento di Scienze e Politiche Ambientali, Università degli Studi di Milano, 20133 Milan, Italy;*

Supplementary statistical methods

15 samples were grouped in three categories, according to: (I) the type of tissue sampled (i.e.: amniotic liquid, placenta and intestine); (II) dam (i.e.: dam A for foetus 1-3, or dam B for foetus 4-5); (III) foetus.

Differences in the microbial communities were evaluated on the basis of biodiversity (α-diversity) and taxonomic composition (β-diversity). Due to the limited number of samples per category, for both α- and β-diversity we applied multiple statistical procedures, flanking the commonly used statistical tests to a strategy based on distributions of distances among samples within and between experimental groups. First, the distance between a single sample against the others was calculated. Then, distances between samples belonging to the same ("intra-category" distance) or to a different ("inter-category" distance) experimental group (i.e.: tissue, dam or foetus) were calculated.

For the α-diversity, we evaluated:

- Results deriving from a MonteCarlo permutation-based, non-parametric t-test;
- Results deriving from the evaluation of the absolute difference for diversity indexes (i.e.: chao1, Shannon index, observed species and Faith's phylogenetic distance). A Mann-Whitney U-test was applied for comparing the distributions of "intra-" and "inter-category" distances.

For the β-diversity, we evaluated:

- The distance matrix partitioning among sources of variations (permutation test with pseudo-F ratios) implemented in the "adonis" test contained in R package "vegan";
- The comparison between distributions of intra- and inter-category Unifrac distances (both weighted or unweighted); the function "make_distance_boxplots.py" in QIIME (http://qiime.org/scripts/make_distance_boxplots.html), implementing a permutation-based non-parametric test on distance distributions, was used to assess a significant clustering among groups.

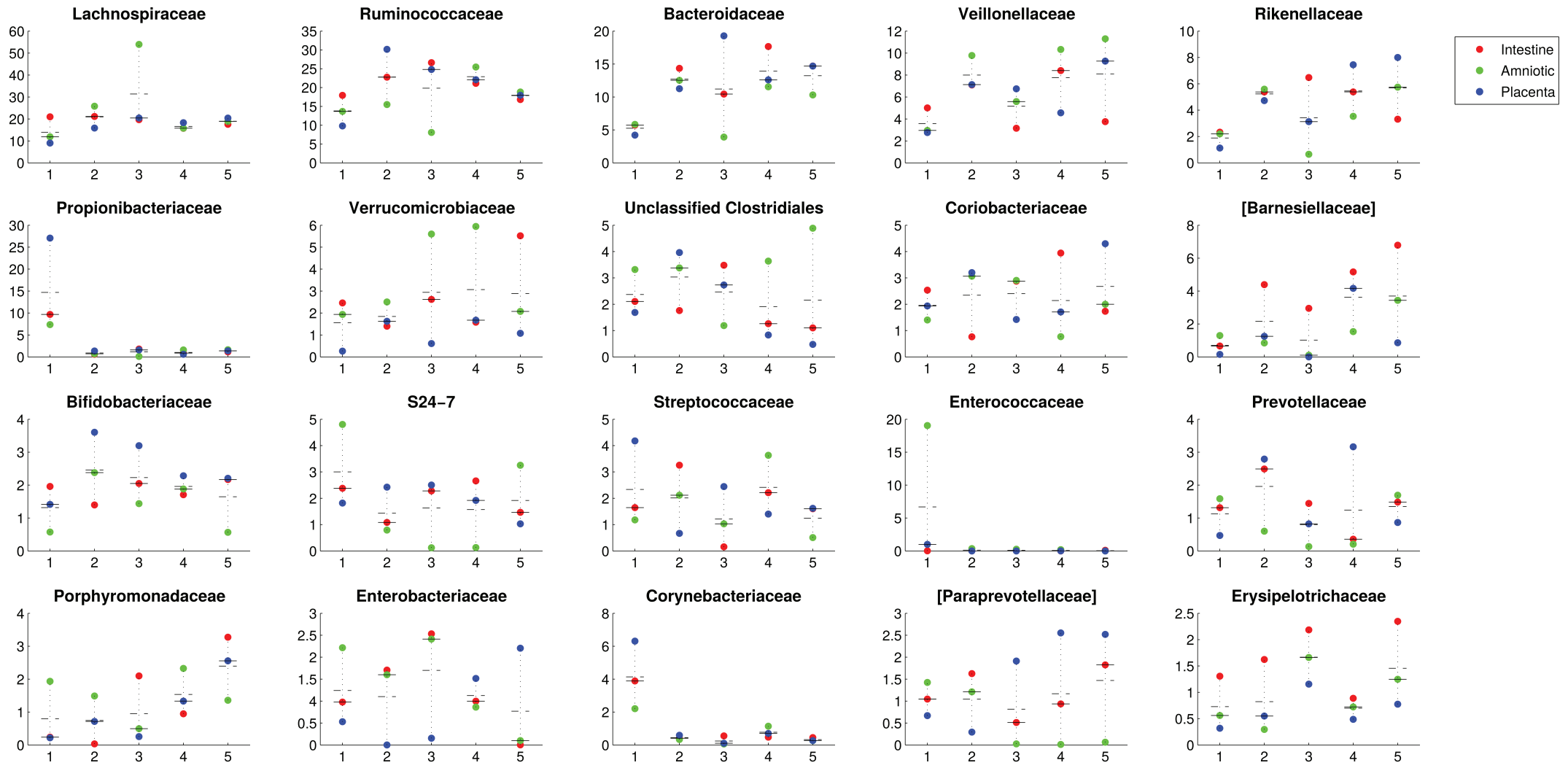

Supplementary figure 1- Relative abundance of most represented bacterial families (per foetus)

Plots show relative abundances of the main 20 bacterial families separated by foetus number. Values corresponding to the same tissue (i.e. intestine, amniotic fluid, and placenta) are represented by the same colour (red, green and blue, respectively). The solid black line represents the median of the values per each foetus, whereas the dashed black line shows the average

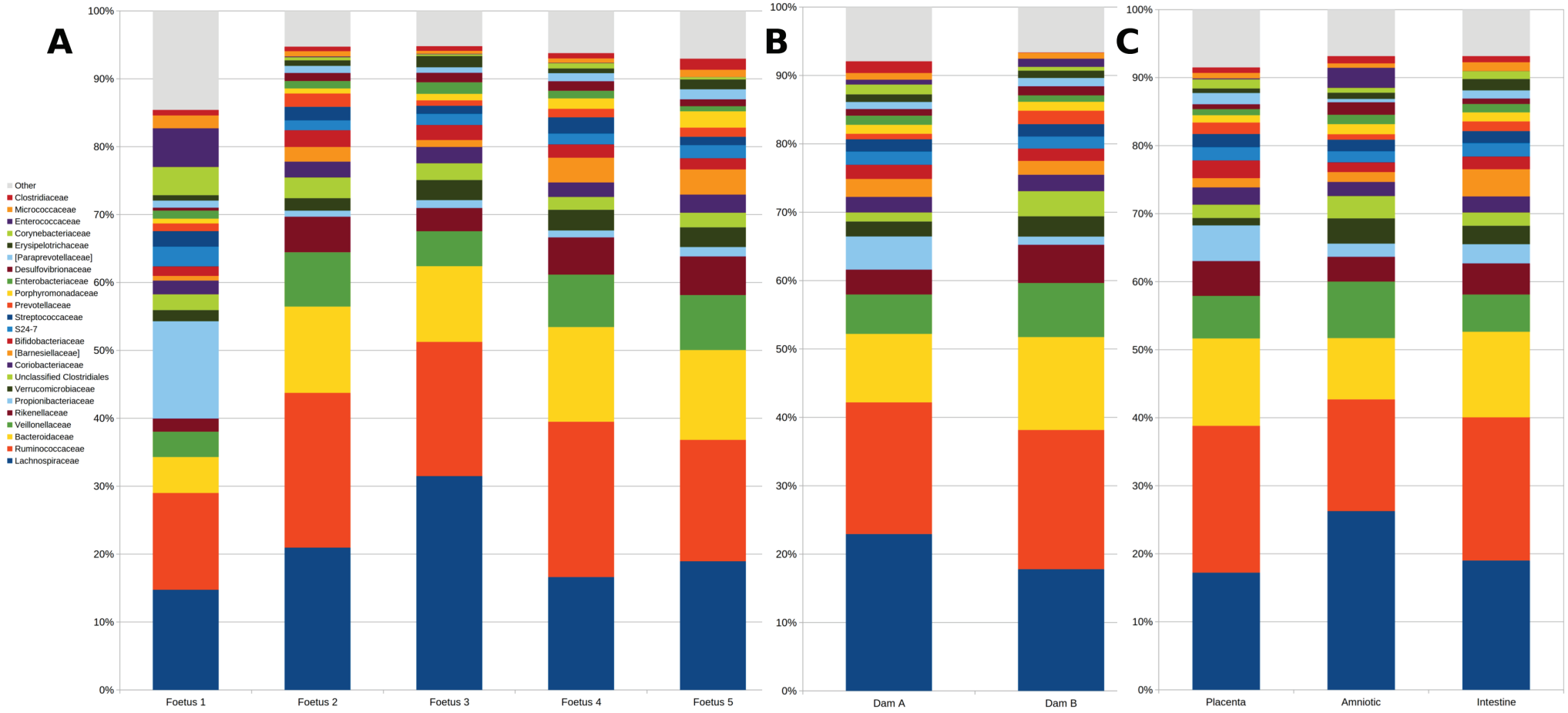

Supplementary figure 2 – Average relative abundance of tissue, dam and foetus microbiota

Average relative abundance of the main microbial families in (A) foetuses, (B) dams and (C) tissues. Samples considered for the analysis were 3 for each foetus, 9 for dam A, 6 for dam B and 5 for each tissue.

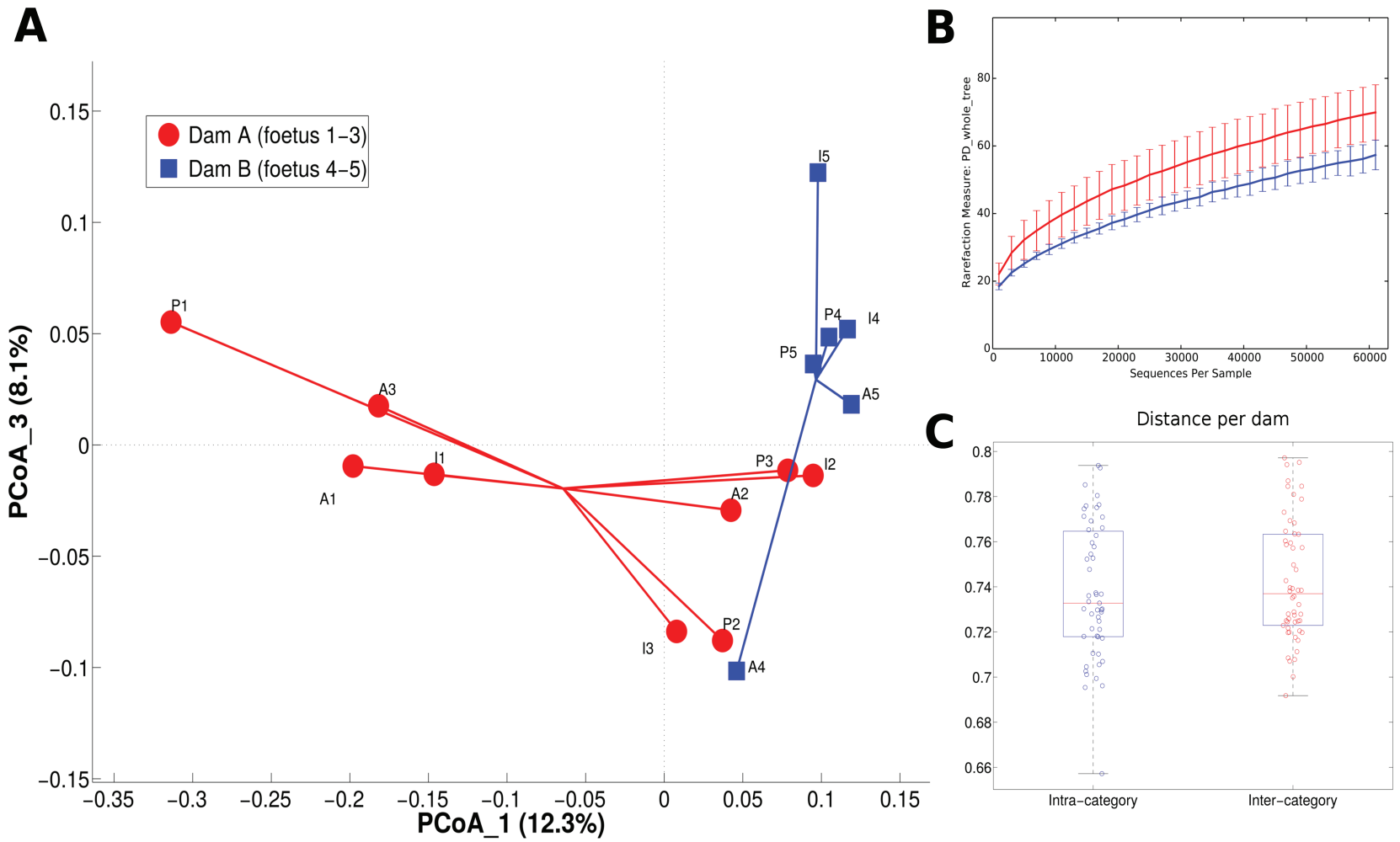

Supplementary figure 3- Dam-effect on microbiota

(A) Principal coordinates analysis (PCoA) of the weighted Unifrac distances; PCoA components 1 and 3 are reported. Samples are grouped based on dam.

(B) Y-axis depicts α-diversity rarefaction curves according to Faith's phylogenetic distance (PD whole tree); numbers of sequences per sample are reported on X-axis.

(C) Boxplots of intra- and inter-category unweighted Unifrac distances among samples; categories are based on dam.

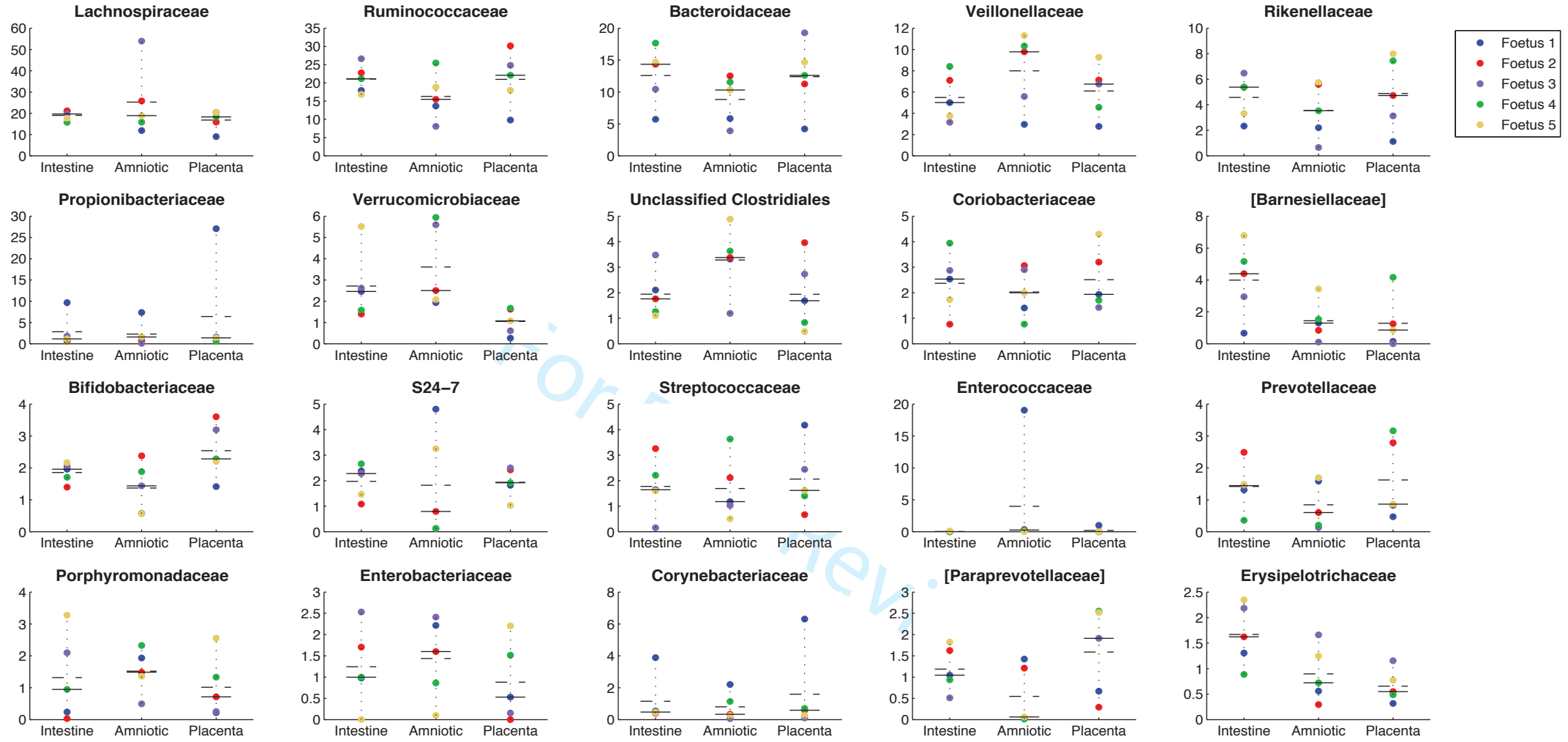

Supplementary figure 4- Relative abundance of most represented bacterial families (per tissue)
Plots show relative abundances of the main 20 bacterial families separated by tissue type. Values corresponding to the same foetus are represented by the same colour. The solid black line represents the median of the values per each tissue, whereas the dashed black line shows the average.

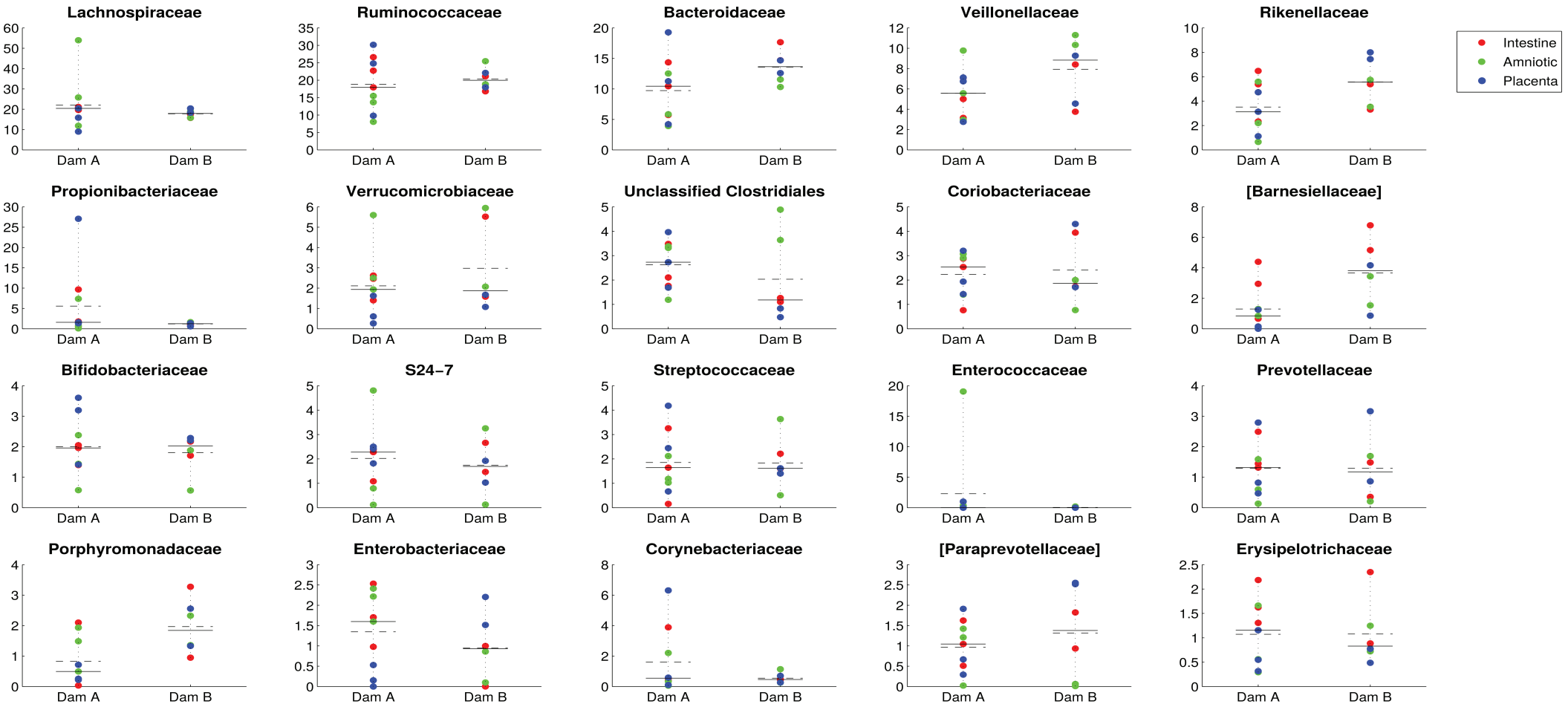

Supplementary figure 5- Relative abundance of most represented bacterial families (per dam)

Plots of relative abundances of the main 20 families of the microbiota separated on dam. Relative abundance corresponding to intestine, amniotic liquid and placenta are represented in red, green and blue, respectively. The solid black line represents the median of the values per each dam, whereas the dashed black line shows the average.

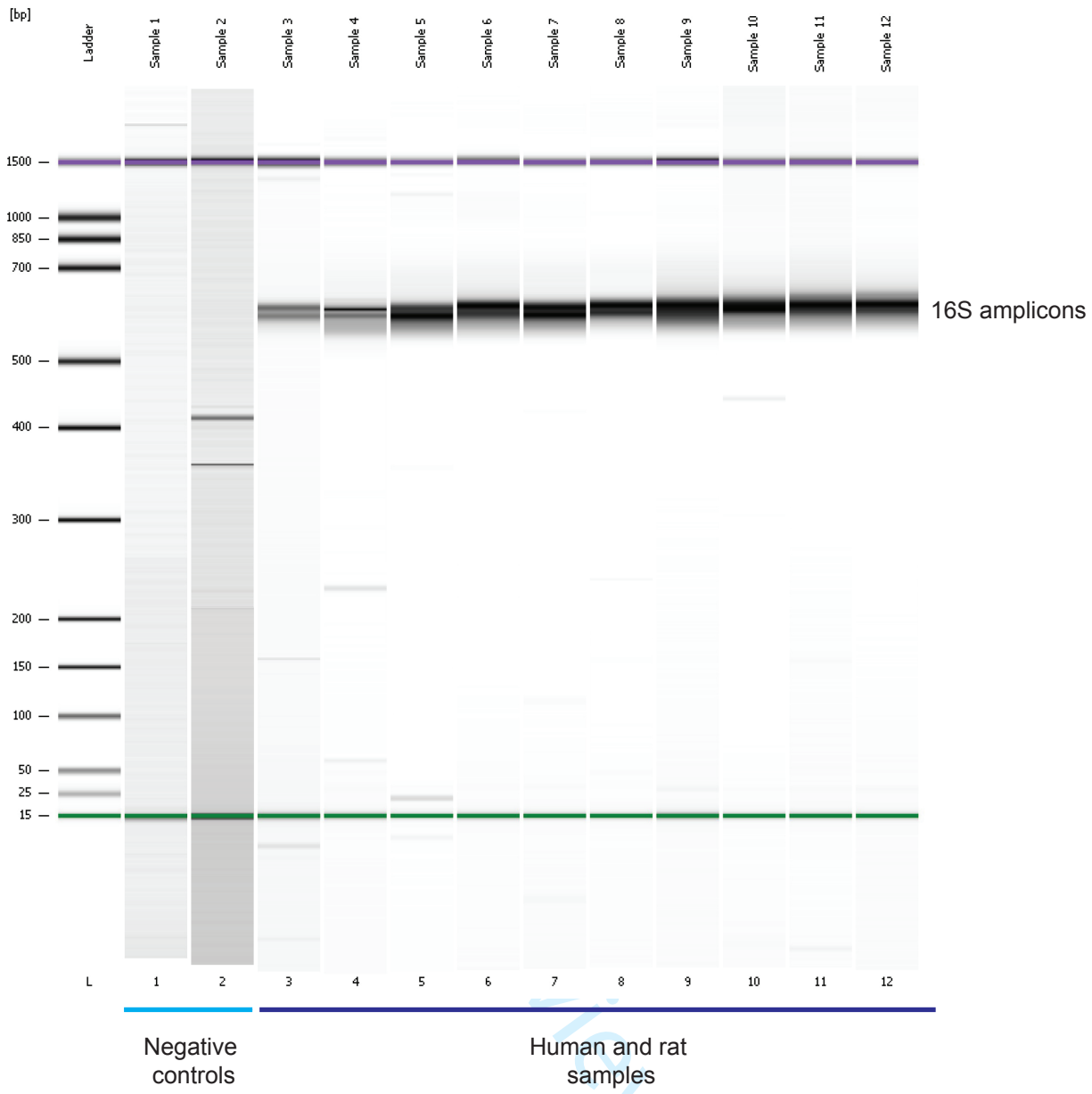

Supplementary figure 6- Representative electrophoresis of 16S amplicons during library check
Agilent 2100 Bioanalyzer system was used to asses exact product size and quantity of amplicons after 16S rRNA gene library preparation, using Agilent DNA 1000 Kit, for the separation, sizing and quantification of dsDNA fragments from 25 to 1000 bp (Agilent Technologies, Santa Clara, CA, USA). First lane (L), molecular weight ladder; lines 1 and 2, negative controls (empty tubes that have been processed in parallel during tissue recovery and DNA extraction); lines 3 to 12, human and rat samples. Upon sequencing, a number of reads to the limit of detection, despite the technical concentration step, has been obtained for negative controls. Known environmental contaminants were never observed.